PHYSICAL REVIEW B **88**, 161201(R) (2013)

Polymorphism of indium oxide: Materials physics of orthorhombic In_2O_3

Aron Walsh*
Centre for Sustainable Chemical Technologies and Department of Chemistry, University of Bath, Claverton Down, Bath BA2 7AY, United Kingdom

David O. Scanlon†
University College London, Kathleen Lonsdale Materials Chemistry, Department of Chemistry, 20 Gordon Street, London, WC1H 0AJ, United Kingdom
and Diamond Light Source Ltd., Diamond House, Harwell Science and Innovation Campus, Didcot, Oxfordshire OX11 0DE, United Kingdom

(Received 20 July 2013; published 9 October 2013)

Indium sesquioxide is the most widely used conductive oxide for optoelectronic applications. The isolation of a novel orthorhombic phase of In_2O_3 at ambient pressures opens a new avenue for tuning the materials properties. Through an explicit comparison of the stable bixbyite and metastable orthorhombic phases of In_2O_3, using a hybrid density functional theory approach, we assess the impact of the loss of inversion symmetry and the distortion of the oxide sublattice on the electronic and defect structure. The band structure of the orthorhombic phase retains the key features of a transparent conductive oxide, with a large separation between the fundamental and optical band gaps. The dominant point defect—the oxygen vacancy—shows similar behavior in both phases with the coexistence of a localized defect wave function in the neutral state and a resonant transition level to the positively charged state. The natural valence band alignment between the cubic and orthorhombic phases is estimated to be 0.22 eV.

DOI: 10.1103/PhysRevB.88.161201 PACS number(s): 61.72.jn, 71.20.−b, 77.84.Bw, 65.40.De

A relatively small number of compounds can be classed as transparent conductive oxides (TCOs), i.e., metal oxides that combine high levels of conductivity and optical transparency in the visible region of the electromagnetic spectrum.[1,2] Of these, indium sesquioxide In_2O_3 is the most ubiquitous,[3] being employed in applications ranging from flat-panel displays to organic photovoltaics. As such, the control and functionalization of the materials properties have attracted a significant amount of attention, ranging from its defect and surface physics[4–13] to interfacial phenomena.[14,15]

Polymorphism describes the existence of multiple crystal structures for a single chemical composition, which may be accessible under the stimulation of pressure and/or temperature. In metal oxides, polymorphs can provide access to a range of physical properties beyond those of the most thermodynamically stable or most common phases, for example, the distinct electron affinity of rutile and anatase structured TiO_2,[16] and the variation in electric dipoles in the perovskite structures of $SrTiO_3$ and $BaTiO_3$.[17–19]

The existence of In_2O_3 polymorphs has long been known. The ground-state cubic bixbyite phase is the most widely studied, while the rhombohedral corundum phase has generated interest due to its stability at modest temperatures and pressures.[20,21] Previous computational work assessed the enthalpic stability of five sesquioxide structures for In_2O_3, and predicted that above 10 GPa the orthorhombic Rh_2O_3 structured phase would be favored.[22] Recently, this transition has been experimentally realized; moreover, the phase remains metastable at ambient pressure and temperature.[23]

In this Rapid Communication, we assess the properties of the new orthorhombic phase of In_2O_3, with comparison to the known cubic phase, using a combination of Born ionic potentials and hybrid density functional theory (DFT). While a number of similarities exist between the phases, the lower formation energy for the oxygen vacancy, combined with a decrease in ionization potential will result in a distinct behavior that could be exploited for future TCO applications.

Computational approach. The properties of crystalline In_2O_3 were calculated first using a set of optimized interatomic potentials,[24] within the code GULP.[25] The resulting structures were then used as the starting point of DFT calculations, as implemented in the code VASP.[26–28] Electron exchange and correlation was treated using the hybrid HSE06 approach,[29] in which 25% of exact nonlocal Hartree-Fock exchange is added to the generalized gradient Perdew-Burke-Ernzerhof functional,[30] and a screening of $\omega = 0.11$ bohr^{-1} is applied to partition the Coulomb potential into short- and long-range terms. The HSE06 functional provides an accurate description of both structural parameters and electronic structure for semiconducting materials.[31,32] The In 4*d* states were included explicitly as valence electrons, and a plane wave cutoff of 520 eV to construct the basis set was found to be well converged with respect to the total energy.

The equilibrium lattice constants were obtained from the energy-volume curves obtained by a series of constant volume calculations, and a fit to the Murnaghan equation of state;[33] the final forces were minimized to below 0.01 eV/Å. The optical transition matrix elements and the optical absorption spectrum were calculated following Fermi's golden rule and within the independent particle approximation, excluding excitonic effects.[34]

Simulation of point defect formation was performed using the supercell approach at the same HSE06-DFT level of theory ($1 \times 2 \times 2$ expansion; 80 atoms) with finite-size corrections, including (i) alignment of the electrostatic potential between the bulk and the defective supercells and (ii) periodic interactions of charged impurities, as outlined by Freysoldt *et al*.[35] The dielectric constants used are those reported in Table I.

TABLE I. Properties of the cubic and orthorhombic polymorphs of In_2O_3 as calculated (at 0 GPa) using an interatomic potential model (detailed in Ref. 22).

Property	Cubic ($Ia\bar{3}$)	Orthorhombic ($Pbcn$)
Lattice constants (Å)	10.117	7.962, 5.477, 5.592
Bulk modulus (GPa)	193.77	210.59
Compressibility ($\times 10^{-3}$ GPa^{-1})	5.16	4.75
Poisson ratio	0.323	0.039 (zy)–0.621 (xy)
Static dielectric constants (ϵ_0)	9.05	15.33, 10.66, 13.80
Optical dielectric constants (ϵ_∞)	3.90	4.47, 4.34, 4.39
Oxygen site potential (V)	22.92	22.70, 22.87
Phonons (cm^{-1})	106–545	96–545

The formation energy of a defect is a function of the chemical environment (atomic chemical potentials). In the oxygen-rich limit, the system is in equilibrium with O_2, while in the oxygen-poor limit, the system is in equilibrium with metallic In. The difference between the two extremes is determined by the formation enthalpy of the compound ($\Delta H_f^{In_2O_3} = -5.98$ eV) following the standard thermodynamic approach.[36]

Crystal structure. The ground-state phase of In_2O_3 is the cubic bixbyite structure (space group $Ia\bar{3}$) which features two distinct In environments that are both coordinated to six oxygen atoms but with S_6 and C_2 symmetry, respectively. The high-pressure orthorhombic structure is based on the high-temperature Rh_2O_3 lattice (space group $Pbcn$), Fig. 1, and contains a single In site. While the cubic phase contains a single oxygen environment (48e Wyckoff position) with tetrahedral coordination, in the orthorhombic phase two different sites exist: the tetrahedral 4c position and the trigonal 8d position. The change in coordination results in a distinct electrostatic environment, with the site Madelung potential of oxygen in the Born potential calculations decreasing by 0.22 V (8d) and 0.05 V (4c) relative to the bixbyite phase.

The predicted bulk materials properties for the cubic and orthorhombic phases, calculated using a polarizable Born

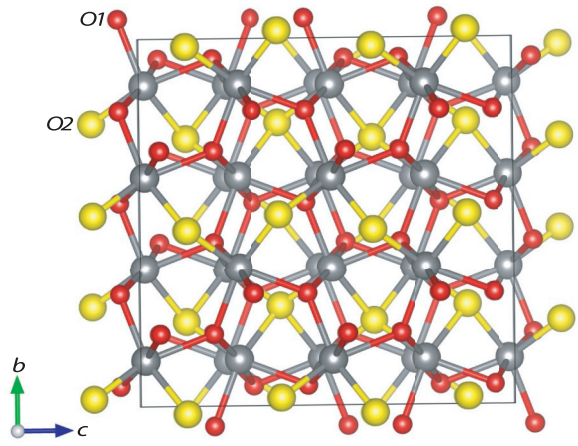

FIG. 1. (Color online) Representation of the crystal structure for the orthorhombic phase of In_2O_3 (1 × 2 × 2 expansion). The two distinct oxygen sites are labeled O1 (8d Wyckoff position) and O2 (4c Wyckoff position).

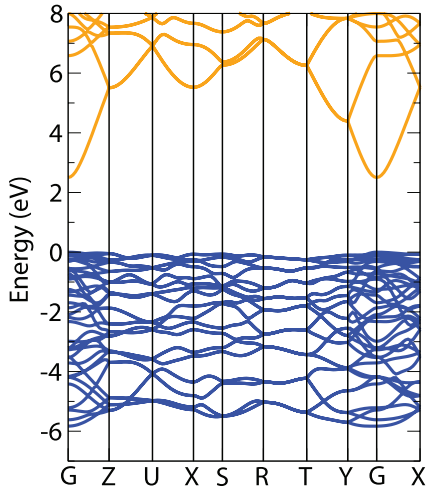

FIG. 2. (Color online) Electronic band dispersion diagram for orthorhombic In_2O_3 calculated at the DFT-HSE06 level of theory. The valence states are colored blue (dark gray), with the conduction states colored yellow (light gray).

potential (previously reported in Ref. 22), are collected in Table I. The lattice constants for both phases are within 1% of those determined experimentally.[23] The HSE06 calculated lattice parameters are $a = 10.157$ Å (cubic phase) and $a = 7.959$ Å, $b = 5.515$ Å, $c = 5.614$ Å (orthorhombic phase), in excellent agreement with the pair-potential calculations. While the mechanical compressibility of the two phases is similar, the dielectric constants are remarkably different, with the orthorhombic phase exhibiting a stronger response at both the low and high frequency limits. The magnitude of the phonon dispersion is similar for both phases.

Electronic structure. The electronic band dispersion in reciprocal space (Fig. 2) maintains the features expected for an n-type TCO: a highly dispersive conduction band with a significant gap between the valence (filled, O 2p derived) and conduction (empty, In 5s derived) bands. At the given level of theory the band gap of the orthorhombic phase (2.50 eV) is 0.13 eV smaller than the cubic phase (2.63 eV). Alignment of the valence band of the bulk materials, with respect to the electrostatic potential of oxygen,[16,37] results in an offset of 0.22 eV. The predicted band alignment is therefore staggered (type II) due to the higher valence band (lower ionization potential) of the orthorhombic phase and the lower conduction band (higher electron affinity) of the cubic phase.

Optical properties. The fundamental band gap of cubic In_2O_3 is dipole forbidden, with strong optical transitions originating from 0.8 eV below the top of the valence band.[38,39] The predicted optical absorption spectrum for orthorhombic In_2O_3 is shown in Fig. 3. Similar behavior is found for the two phases despite the fact that the crystal structure of orthorhombic In_2O_3 contains no center of inversion. Therefore, while low energy valence to conduction band transitions are not formally forbidden by the wave function symmetry, they remain of negligible intensity.

Defect physics. It has been established that oxygen vacancies are the dominant intrinsic defect in this class of metal oxide.[7–9,11–13,22,40] The role of adventitious hydrogen in bulk conductivity is more controversial.[41,42] There has been intense

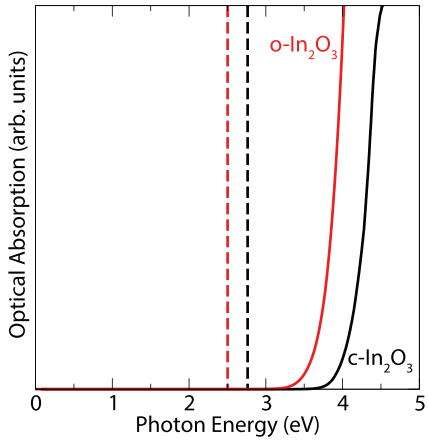

FIG. 3. (Color online) Predicted optical absorption onset for orthorhombic [red (light gray) lines] and cubic (black lines) In_2O_3. Only vertical one-electron transitions are considered. The dashed vertical lines represent the fundamental band gaps as determined from the electronic band structure.

debate relating to the behavior of the oxygen vacancy, i.e., the degree of localization and the ionization energy to a charged state. There have been reports of both shallow and deep donor characteristics for V_O, even where similar methods were employed.[43,44]

The formation of an oxygen vacancy can be separated into two processes. First, the energy required to produce a neutral oxygen vacancy in the lattice, chemically balanced with respect to gaseous oxygen (spin triplet configuration):

$$O_O \rightleftharpoons V_O^{\times} + \tfrac{1}{2}O_2(g). \tag{1}$$

This process gives rise to two excess electrons (due to the absence of the oxide anion), which are strongly localized in the vacancy center, similar to the color centers found in alkali halides (Fig. 4). Secondly, the thermal (or optical) ionization of the neutral defect to generate two free carriers in the conduction

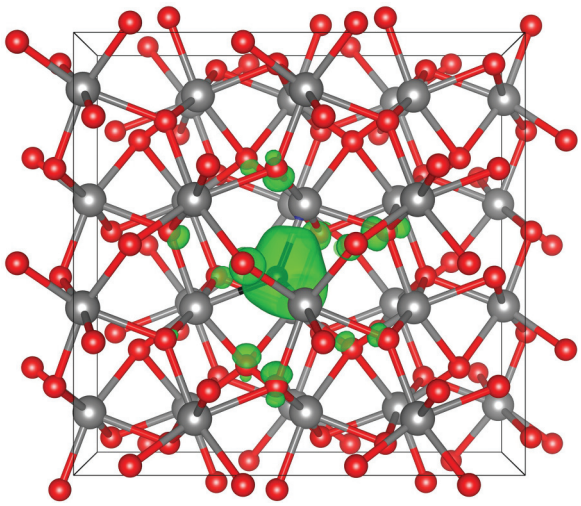

FIG. 4. (Color online) Electron density arising from the occupied defect band in oxygen-deficient o-In_2O_3 for the 8*d* oxygen site (the plot for 4*c* is similar). The results were obtained using an 80 atom supercell and the HSE06 functional.

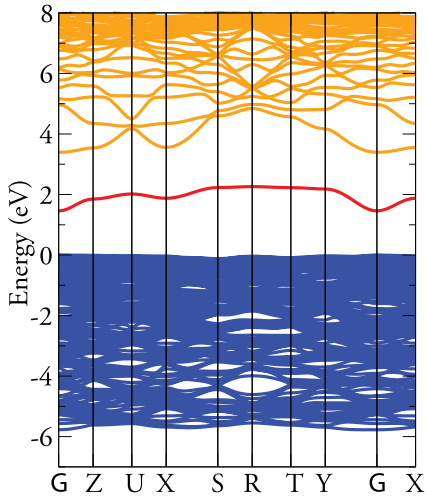

FIG. 5. (Color online) Electronic band structure for a supercell of orthorhombic In_2O_3 containing an oxygen vacancy defect. While the lattice symmetry is broken upon defect formation, the dispersion across the first Brillouin zone is shown for illustrative purposes. The top of the valence band is set to 0 eV, while the occupied vacancy band can be found at ∼2 eV.

band can occur:

$$V_O^{\times} \rightarrow V_O^{\bullet\bullet} + 2e'. \tag{2}$$

Equation (2) can be further separated into two single-electron ionization processes, but as given it represents total ionization of the defect band. We have computed the formation energies of the neutral oxygen vacancies to be 3.34 and 3.36 eV for the 8*d* and 4*c* sites, respectively. Under reducing conditions, these lower to ∼1.3 eV, in line with previous reports for the cubic phase.[11] The corresponding $(0/+2)$ ionization levels for the 8*d* and 4*c* oxygen vacancies are 2.59 and 2.74 eV above the top of the valence band, placing them in the conduction band, consistent with a resonant donor defect. These are adiabatic ionization energies, which in contrast to the one-electron band structure represent quasiparticle energies to promote electrons from the defect state to the conduction band of the host material and include structural relaxation of the initial and final states.

The behavior of the oxygen vacancy defect in In_2O_3 is complicated by the fact that it combines both a localized wave function (Fig. 4) and deep single-particle level (Fig. 5) with a low energy of ionization. The results obtained for orthorhombic In_2O_3 are consistent with the arguments of both Lany and Zunger[43] *and* Ágoston *et al.*[44] for the cubic phase. While the oxygen vacancy is predicted to be a resonant donor at this level of theory, the large relaxation between the neutral and doubly ionized configurations would be expected to give rise to a kinetic barrier for the electron transfer process.

In conclusion, we have elucidated the properties of a new phase of In_2O_3, which has similar but distinct bulk properties and defect behavior compared to the common cubic phase. Beyond this material, the work emphasizes the importance of polymorphism for metal oxides, and indeed in many semiconductor compounds [e.g., $ZnSnP_2$,[45] $ZnSnN_2$,[46] $SrGeO_3$ (Ref. 47)], where the crystal structure can be used

to tune the materials properties. It provides an opportunity to change the behavior of a material without changing its chemical composition.

Acknowledgments. We acknowledge support from the HPC Materials Chemistry Consortium, which is funded by EPSRC (EP/F067496), and the Materials Design Network. D.O.S. is grateful to the Ramsay Memorial Trust and University College London for the support of a Ramsay fellowship. A.W. acknowledges support from the Royal Society through a University Research fellowship.

*a.walsh@bath.ac.uk

†d.scanlon@ucl.ac.uk

[1]P. P. Edwards, A. Porch, M. O. Jones, D. V. Morgan, and R. M. Perks, Dalton Trans. **15**, 2995 (2004).

[2]P. D. C. King and T. D. Veal, J. Phys.: Condens. Matter **23**, 334214 (2011).

[3]I. Hamberg, C. G. Granqvist, K. F. Berggren, B. E. Sernelius, and L. Engstrom, Phys. Rev. B **30**, 3240 (1984).

[4]Y. Ohya, T. Yamamoto, and T. Ban, J. Am. Ceram. Soc. **91**, 240 (2007).

[5]J. H. W. DeWit, J. Solid State Chem. **20**, 143 (1977).

[6]R. L. Weiher, J. Appl. Phys. **33**, 2834 (1962).

[7]S. Lany and A. Zunger, Phys. Rev. Lett. **98**, 045501 (2007).

[8]T. Tomita, K. Yamashita, Y. Hayafuji, and H. Adachi, Appl. Phys. Lett. **87**, 051911 (2005).

[9]P. Ágoston, K. Albe, R. M. Nieminen, and M. J. Puska, Phys. Rev. Lett. **103**, 245501 (2009).

[10]A. Walsh, J. L. F. Da Silva, and S.-H. Wei, Phys. Rev. B **78**, 075211 (2008).

[11]P. Ágoston, P. Erhart, A. Klein, and K. Albe, J. Phys.: Condens. Matter **21**, 455801 (2009).

[12]J. E. Medvedeva and C. L. Hettiarachchi, Phys. Rev. B **81**, 125116 (2010).

[13]A. Walsh, Appl. Phys. Lett. **98**, 261910 (2011).

[14]A. Walsh, C. R. A. Catlow, K. H. L. Zhang, and R. G. Egdell, Phys. Rev. B **83**, 161202 (2011).

[15]F. Rüggeberg and A. Klein, Appl. Phys. A **82**, 281 (2005).

[16]D. O. Scanlon, C. W. Dunnill, J. Buckeridge, S. A. Shevlin, A. J. Logsdail, S. M. Woodley, C. R. A. Catlow, M. J. Powell, R. G. Palgrave, I. P. Parkin *et al*., Nat. Mater. **12**, 798 (2013).

[17]R. Ramesh and N. A. Spaldin, Nat. Mater. **6**, 21 (2007).

[18]A. M. Glazer, Acta Crystallogr., Sect. B: Struct. Crystallogr. Cryst. Chem. **28**, 3384 (1972).

[19]C. R. A. Catlow, Z. X. Guo, M. Miskufova, S. A. Shevlin, A. G. H. Smith, A. A. Sokol, A. Walsh, D. J. Wilson, and S. M. Woodley, Philos. Trans. R. Soc. London, Ser. A **368**, 3379 (2010).

[20]S. Z. Karazhanov, P. Ravindran, P. Vajeeston, A. Ulyashin, T. G. Finstad, and H. Fjellvag, Phys. Rev. B **76**, 075129 (2007).

[21]P. D. C. King, T. D. Veal, F. Fuchs, C. Y. Wang, D. J. Payne, A. Bourlange, H. Zhang, G. R. Bell, V. Cimalla, O. Ambacher, R. G. Egdell, F. Bechstedt, and C. F. McConville, Phys. Rev. B **79**, 205211 (2009).

[22]A. Walsh, C. R. A. Catlow, A. A. Sokol, and S. M. Woodley, Chem. Mater. **21**, 4962 (2009).

[23]M. F. Bekheet, M. R. Schwarz, S. Lauterbach, H.-J. Kleebe, P. Kroll, R. Riedel, and A. Gurlo, Angew. Chem. **52**, 6531 (2013).

[24]A. Walsh, S. M. Woodley, C. R. A. Catlow, and A. A. Sokol, Solid State Ionics **184**, 52 (2011).

[25]J. D. Gale and A. L. Rohl, Mol. Simul. **29**, 291 (2003).

[26]G. Kresse and J. Furthmüller, Phys. Rev. B **54**, 11169 (1996).

[27]G. Kresse and J. Furthmüller, Comput. Mater. Sci. **6**, 15 (1996).

[28]G. Kresse and D. Joubert, Phys. Rev. B **59**, 1758 (1999).

[29]J. Heyd, G. E. Scuseria, and M. Ernzerhof, J. Chem. Phys. **118**, 8207 (2003).

[30]J. P. Perdew, K. Burke, and M. Ernzerhof, Phys. Rev. Lett. **77**, 3865 (1996).

[31]J. Heyd, J. E. Peralta, G. E. Scuseria, and R. L. Martin, J. Chem. Phys. **123**, 174101 (2005).

[32]D. O. Scanlon, A. B. Kehoe, G. W. Watson, M. O. Jones, W. I. F. David, D. J. Payne, R. G. Edgell, P. P. Edwards, and A. Walsh, Phys. Rev. Lett. **107**, 246402 (2011).

[33]F. D. Murnaghan, Proc. Natl. Acad. Sci. U.S.A. **30**, 244 (1944).

[34]B. Adolph, J. Furthmüller, and F. Bechstedt, Phys. Rev. B **63**, 125108 (2001).

[35]C. Freysoldt, J. Neugebauer, and C. G. Van de Walle, Phys. Rev. Lett. **102**, 016402 (2009).

[36]J. Buckeridge, D. O. Scanlon, A. Walsh, and C. R. A. Catlow, Comput. Phys. Commun. (2013), http://dx.doi.org/10.1016/j.cpc.2013.08.026.

[37]N. F. Mott and R. W. Gurney, *Electronic Processes in Ionic Crystals*, 2nd ed. (Oxford University Press, Oxford, 1948).

[38]A. Walsh, J. L. F. Da Silva, S.-H. Wei, C. Körber, A. Klein, L. F. J. Piper, A. DeMasi, K. E. Smith, G. Panaccione, P. Torelli, D. J. Payne, A. Bourlange, and R. G. Egdell, Phys. Rev. Lett. **100**, 167402 (2008).

[39]F. Fuchs and F. Bechstedt, Phys. Rev. B **77**, 155107 (2008).

[40]M. Burbano, D. O. Scanlon, and G. W. Watson, J. Am. Chem. Soc. **133**, 15065 (2011).

[41]P. D. C. King, R. L. Lichti, Y. G. Celebi, J. M. Gil, R. C. Vilão, H. V. Alberto, J. Piroto Duarte, D. J. Payne, R. G. Egdell, I. McKenzie, C. F. McConville, S. F. J. Cox, and T. D. Veal, Phys. Rev. B **80**, 081201 (2009).

[42]S. Limpijumnong, P. Reunchan, A. Janotti, and C. G. Van de Walle, Phys. Rev. B **80**, 193202 (2009).

[43]S. Lany and A. Zunger, Phys. Rev. Lett. **106**, 069601 (2011).

[44]P. Ágoston, K. Albe, R. M. Nieminen, and M. J. Puska, Phys. Rev. Lett. **106**, 069602 (2011).

[45]D. O. Scanlon and A. Walsh, Appl. Phys. Lett. **100**, 251911 (2012).

[46]N. Feldberg, J. D. Aldous, W. M. Linhart, L. J. Philips, K. Durose, P. A. Stampe, R. J. Kennedy, D. O. Scanlon, G. Vardar, R. L. Field, III, T. Y. Jen, R. S. Goldman, T. D. Veal, and S. M. Durbin, Appl. Phys. Lett. **103**, 042109 (2013).

[47]H. Mizoguchi, T. Kamiya, S. Matsuishi, and H. Hosono, Nat. Commun. **2**, 470 (2011).